ANALYSIS OF THE FUNCTION OF MATRIX ATTACHMENT REGION-BINDING FILAMENT-LIKE PROTEIN 1 (MFP1) IN THE CHLOROPLAST THYLAKOID MEMBRANE OF *ARABIDOPSIS THALIANA*

A Thesis
by
AMANDA ROSE HAVIGHORST

Submitted to the Graduate School
Appalachian State University
in partial fulfillment of the requirements for the degree of
MASTER OF SCIENCE

December 2012
Department of Biology

ANALYSIS OF THE FUNCTION OF MATRIX ATTACHMENT REGION-BINDING FILAMENT-LIKE PROTEIN 1 (MFP1) IN THE CHLOROPLAST THYLAKOID MEMBRANE OF *ARABIDOPSIS THALIANA*

A Thesis
by
AMANDA ROSE HAVIGHORST
December 2012

APPROVED BY:

_____
Annkatrin Rose
Chairperson, Thesis Committee

_____
Mary U. Connell
Member, Thesis Committee

_____
Mark Venable
Member, Thesis Committee

_____
Susan L. Edwards
Chairperson, Department of Biology

_____
Edelma Huntley
Dean, Research and Graduate Studies

ABSTRACT

ANALYSIS OF THE FUNCTION OF MATRIX ATTACHMENT REGION-BINDING FILAMENT-LIKE PROTEIN 1 (MFP1) IN THE CHLOROPLAST THYLAKOID MEMBRANE OF *ARABIDOPSIS THALIANA*
(Dec. 2012)

Amanda Rose Havighorst, B.S., Western Carolina University

M.S., Appalachian State University

Chairperson: Annkatrin Rose

Matrix Attachment Region-Binding Filament-Like Protein 1 (MFP1) is a DNA-binding long coiled-coil plant protein with a structure similar to that of the golgins of the Golgi apparatus, which aid in maintaining the organelle's characteristic membrane stacks. Though initially believed to be associated with the nuclear matrix, it was later found to localize to the chloroplast and embed itself in the thylakoid membrane, the location of the proteins responsible for the photosynthetic light reactions. The thylakoid membranes of higher-plant chloroplasts exhibit a stacked structure very similar in appearance to that of the Golgi apparatus, and MFP1 has only been found in higher plants. Due to the similarities in the protein structure of MFP1 and golgins, and the similarities in structure between the Golgi apparatus and the thylakoid membrane, we hypothesized that MFP1 had a function like that of the golgins: facilitating the formation of the thylakoid grana stacks. *Arabidopsis thaliana* mutants lacking MFP1 were examined for phenotypic

differences, both on the macroscopic scale (growth rate, color, rosette density and size) and on the microscopic scale (thylakoid membrane stacking ability), as well as on the molecular scale (chlorophyll content, protein complexes). Under ideal lighting conditions, the mutants did not appear any different from the wild-type, but when exposed to differing light conditions, the phenotype was expressed in the form of slower growth and a denser, slightly larger rosette. Transmission electron microscopy revealed little difference in the grana stacks between the wild-type and the mutant, and no significant difference in chlorophyll content. Blue Native Polyacrylamide Gel Electrophoresis revealed a possible association between MFP1 and the Light Harvesting Complex II (LHCII), an important component of the photosynthetic machinery. This apparent association along with the light-induced phenotype suggest that MFP1 may play some role in photosynthetic adaptation, either in state transitioning (movement of LHCII to Photosystem I) or in adjusting the photosystem stoichiometry (changing the ratio of Photosystem I to Photosystem II).

ACKNOWLEDGEMENTS

I would like to thank Dr. Annkatrin Rose, my advisor, for accepting me into her lab and for her assistance in completing my research. I would also like to thank my committee members, Dr. Mary U. Connell and Dr. Mark Venable, for their time and contributions to my research and to my thesis. Additionally, I would like to thank Dr. Guichuan Hou for allowing me to work in the microscopy facility and for training me in electron microscopy sample preparation, and the use of the microtome and transmission electron microscope, and Dr. Howard Neufeld for his suggestions on where next to take my research.

I would like to thank Alison DeShields for her assistance in the statistical analysis of the chlorophyll count data, and the rest of the Rose Lab and the biology department for their friendship and support. I am also grateful to my family for their love, especially my mother for her emotional support, and my father for his interest in and support of my work.

I would like to thank the Department of Biology for providing funds for my work, and I would finally like to extend special thanks to the Office of Student Research, for without their funding, I would not have been able to perform the critical Blue-Native PAGE analysis that made my thesis what it is today.

TABLE OF CONTENTS

LIST OF FIGURES

Page

INTRODUCTION

Photosynthesis is the process by which energy from light is converted from solar radiation into a chemical form usable by an organism (Anderson 1982). This process is vital not only to the photosynthetic organisms which utilize it, but also to fungi and animals, including humans, which depend on photosynthetic organisms for food and oxygen. While there are both oxygenic and anoxygenic photosyntheses, it is oxygenic photosynthesis which makes life on Earth as we know it possible. Organisms performing oxygenic photosynthesis are responsible for not only the production of sugars and other nutrients which are distributed throughout the world's food chains, but also for the production of oxygen, which is necessary for the survival of aerobic organisms.

Photosynthesis occurs in two phases: the "light" reactions, during which sunlight is harnessed to produce ATP and NADPH; and the "dark" reactions, also known as the Calvin Cycle, in which the ATP and NADPH are used in the fixation of carbon and in the production of various biomolecules. Light is gathered by Photosystem II (PSII), Photosystem I (PSI), and by the large antennae complexes made up of Light Harvesting Complex proteins (LHC) which funnel the energy to the reaction centers of the photosystems. PSII, functionally the "first" of the photosystems in the chain, uses water as an electron donor, and uses the light energy to split water molecules, producing protons and oxygen. The electron from water is then passed on to pheophytin, followed by plastoquinone, before reaching the cytochrome b_6f complex. The cytochrome b_6f

complex transfers this electron to plastocyanin and pumps extra protons into the thylakoid lumen. The electron is moved from plastocyanin to PSI. From PSI, the electron is accepted by ferredoxin, and finally by $NADP^+$ reductase, which transfers electrons to $NADP^+$, which is reduced to NADPH. Meanwhile, the proton gradient generated by PSII's oxidation of water and the cytochrome b_6f proton pump causes the protons to shoot through ATP synthase, which converts ADP into ATP. The generated NADPH and ATP are then fed into the Calvin cycle, which fixes carbon to form carbohydrates (Sharkey 1985).

In eukaryotes, photosynthesis occurs in the chloroplasts, which are organelles found only in plants, algae, and other photosynthetic protists. It is likely that the chloroplasts originated from photosynthetic prokaryotes called cyanobacteria, which were engulfed by a primitive eukaryotic cell and became endosymbionts (Jaynes and Vernon 1982; Cattolico 1986; Shih et al. 1986; Giovannoni et al. 1988; Mamedov et al. 1991; Lemieux et al. 1999; Cavalier-Smith 2002; Raven and Allen 2003; Peltier et al. 2004). After endosymbiosis, genes from the cyanobacteria were transferred to the nucleus of the eukaryotic cell, effectively making the cyanobacterium reliant on the plant cell; chloroplasts can no longer survive on their own (Martin et al. 1998; Martin et al. 2002). Evidence of this cyanobacterial ancestry is seen in some types of algae. Glaucophytes, for example, produce chloroplast-like plastids called "cyanelles" which retain distinctly cyanobacterial features, such as a peptidoglycan cell wall, that are absent in higher plant chloroplasts (Raven 2002).

Cyanobacteria and the chloroplasts of photosynthetic eukaryotes contain membranes known as thylakoid membranes (Tester and Blatt 1989). Numerous studies

show that the thylakoid is where the light reactions occur, and thus it is the location of proteins which are necessary for these reactions (Rippka et al. 1974; Anderson 1982; Bald et al. 1996; Allen and Forsberg 2001; Schubert et al. 2002; Shimoni et al. 2005). The light reactions occur across the surface of the thylakoid membrane, while the Calvin cycle occurs in the stroma, outside of the thylakoid membrane (Tester and Blatt 1989).

Thylakoid membranes vary in structure, depending on the type of organism they are found in. In cyanobacteria, the thylakoid is flat, and is found associated with the cell membrane (Vothknecht and Westhoff 2001). In plant chloroplasts, the thylakoid consists of stacks called grana stacks, as well as unstacked sections of membrane called lamellae that are exposed to the stroma (Anderson and Melis 1983; Kramer et al. 1988; Vothknecht and Westhoff 2001; Trissl and Wilhelm 2002). Some proteins and protein complexes, primarily PSII and its associated light-harvesting complex LHCII, are concentrated within the grana stacks, while others, such as PSI and ATP synthase, are located in the lamellae, separated from PSII to prevent excitation spillover (Simpson and Wettstein 1989). Cytochrome b_6f is evenly distributed throughout the thylakoid membrane, as it plays a role both in linear electron flow and cyclic electron flow. It is also possible for LHCII to move out of the thylakoid membrane during a state transition, under PSII-favoring light conditions. Because of the presence of PSII and LHCII, 80% of the chlorophyll in a chloroplast is located in these grana stacks under normal light conditions (Albertsson 2001).

Many different factors go into forming the thylakoid membranes. The lipid composition of the chloroplast envelope is different from the lipid composition of the thylakoid membrane. The galactolipids monogalactosyldiacylglycerol (MGDG) and

digalactosyldiacylglycerol (DGDG) must be produced by enzymes within the chloroplast envelope and account for 75% of the total lipids in the thylakoid membrane. Evidence suggests that they play an important role in the photosynthetic reactions (Andersson et al. 2001; Kobayashi et al. 2007). Plants that lack MGDG and DGDG can neither form thylakoid membranes nor photosynthesize (Kobayashi et al. 2007). While the chloroplast retains some genes, many chloroplast proteins necessary for thylakoid biogenesis and for photosynthesis, such as components of the photosystems and LHCII, are encoded in the nucleus of the plant cell. Nuclear-encoded chloroplast proteins are made in the cytosol with chloroplast targeting signals, and then must be transported into the developing chloroplast (Hoober and Eggink 1999; Kroll et al. 2000). Once inside the chloroplast, the targeting regions are removed and the protein subunits are assembled into their appropriate complexes (Hoober and Eggink 1999).

Currently, it is thought that trimeric LHCII is needed for grana stacks to form properly (Cui et al. 2011). Plants lacking the LHCII trimer fail to form substantial grana stacks, and experiments demonstrate that reintroducing LHCII into membranes which lack them restores the plant's ability to form grana stacks (Cui et al. 2011). In the Golgi bodies, an organelle which exhibits a similarly stacked structure, the stacking is facilitated by the presence of golgins (Rose et al. 2004). Golgins are the proteins which hold together the sections of the Golgi body, called cisternae, by forming proteinaceous bridges that link them together (Barr and Short 2003; Short et al. 2004). The golgins exhibit a long coiled-coil domain that forms a rodlike structure; these proteins connect to each other and maintain the structure of the Golgi body (Barr and Short 2003). Like the

Golgi body, the thylakoid membrane is a dynamic structure that can stack and unstack itself as necessary (Short et al. 2004; Pfeiffer and Krupinska 2005).

Coiled-coil proteins are found in most organisms, including in prokaryotes. Their structure, consisting of two alpha-helices that wrap around each other, is facilitated by a heptad repeat, in which the first and fourth residues are hydrophobic, while the fifth and seventh are hydrophilic (Rose and Meier 2004). The hydrophobic side chains of two monomers interact with each other, forming the distinctive "coiled-coil" structure (Rose and Meier 2004). The number of heptad repeats varies from protein to protein, and the number of monomers in a protein can vary, meaning that coiled-coil proteins are highly diverse and versatile (Rose and Meier 2004).

Coiled-coil proteins have many different functions in a variety of locations in the cell. A number of transcription factors have short coiled-coil regions referred to as leucine zippers (Rose and Meier 2004). Small coiled-coil proteins are also important in signal transduction pathways, such as the *iguana* gene product Dzip1, which is a part of the Hedgehog signaling pathway essential for proper embryo formation in many animals (Wolff et al. 2003). Long coiled-coil proteins, such as the golgins, play other roles, including the formation of cytoskeletal networks, structural maintenance of chromosomes (Smc) proteins which organize chromatin within the nucleus, and the nuclear lamins, which attach the chromatin to the nuclear envelope (Rose and Meier 2004). While long coiled-coil proteins are common and well-studied in animals, they are not so common in plants, and only a few of those that are present have been studied (Rose and Meier 2004).

Matrix attachment region-binding filament-like protein 1 (MFP1) is a DNA-binding coiled-coil protein, structurally similar to golgins, which is located in the

thylakoid membranes of the chloroplasts in plants and is also associated with the nucleoids in the chloroplasts (Jeong et al. 2003). It was originally predicted by Gindullis and Meier (1999) to be associated with the endoplasmic reticulum, or as part of the nuclear envelope, but was later found to contain a signal peptide that is normally characteristic of import into the chloroplast and subsequent thylakoid localization (Jeong et al. 2003; Samaniego et al. 2006). It is also structurally similar to the nuclear lamins of animal cells, which connect the chromatin to the nuclear envelope (Jeong et al. 2003). Plant cells do not have nuclear lamins, but its ability to bind DNA, its attachment to a membrane, and the fact that it is a long coiled-coil protein make them similar (Jeong et al. 2003). While the function of MFP1 as of now remains unknown, the fact that stacking mechanisms in organelles like the Golgi body are facilitated by long coiled-coil proteins like MFP1 led me to hypothesize that the protein may have a function similar to that of the golgins.

The gene that encodes MFP1 contains four exons separated by three relatively short introns. The final mRNA sequence is 2,537 base pairs long. The protein that it encodes is 726 amino acids long (NCBI, accession number NP_188221). While it is found in several species, the overall degree of conservation of the MFP1 sequence between species is very low. There are several domains, however, that remain conserved (Samaniego et al. 2008). Some plants it is found in include Arabidopsis (*Arabidopsis thaliana*), tomato (*Solanum lycopersicum*), a tobacco species (*Nicotiana benthamiana*), rice (*Oryza sativa*), soybean (*Glycine max*), corn (*Zea mays*), and wheat (*Triticum aestivum*), and several others which are not listed here (Harder *et al.* 2000).

Gene expression studies show that the period of chloroplast development is also the period that MFP1 begins to accumulate (Jeong et al. 2003, 2004). Likewise, MFP1 expression is highest when light is present, and in the shoots of the plant, where photosynthesis occurs; it is lowest in the dark and in non-photosynthetic areas (Samaniego et al. 2006). Most of the MFP1 produced by the cell is located in the thylakoid membrane of the chloroplast, on the stroma side, which is where the carbohydrate formation reaction powered by photosynthesis occurs (Jeong et al. 2004; Samaniego et al. 2006). This location and orientation is optimal for a protein with a role in thylakoid stacking.

The objective of my study was to elucidate a possible function for MFP1. I used an MFP1 knockout mutant generated via agrobacterial T-DNA insertion (Jeong et al. 2003) for my experiments. This mutant does not express MFP1 at all, and the T-DNA is inserted between the second and third exon (Jeong et al. 2003). This allowed me to examine the effects of MFP1's absence on the plant's ability to photosynthesize, produce chloroplasts, and produce grana stacks.

Plants were observed on both the macroscopic and microscopic scale, using transmission electron microscopy to directly view the thylakoid membranes and light microscopy to look at chloroplast morphology and abundance. Plants were also examined on the molecular scale, using Blue-Native Polyacrylamide Gel Electrophoresis (BN-PAGE) to analyze the states of important chloroplast protein complexes and to search for a possible association between MFP1 and the photosynthetic complexes (PSII, PSI, etc.).

MATERIALS AND METHODS

Plants and Growth Conditions

The plants used include Wild-Type (WT) Arabidopsis plants (WS ecotype) and the T-DNA knockout mutant K-8-5, which cannot produce MFP1 (Jeong et al. 2003). Seeds of K-8-5 and WT plants were sterilized using a solution containing 2 mL 6% hypochlorite solution (Clorox brand), 1 µL TWEEN (Sigma-Aldrich Co., St. Louis, MO, USA), and 10 mL deionized water. Seeds were initially washed in 500 µL sterilization solution for 10 minutes. The seeds were briefly centrifuged in a microcentrifuge at 16,100 x *g* (Eppendorf Centrifuge 5415 D, Eppendorf International, Hamburg, Germany), the sterilization solution was removed, and 500 µL of sterile water was added. The seeds were then placed on a rocker (Lab-Line Maxi-Rotator 4631, Barnstead International, Dubuque, IA, USA) for two minutes, centrifuged, and another 500 µL water was added; this was repeated five times. Once sterilized, the seeds were placed on Petri plates containing Gamborg's medium.

The Gamborg's medium was made using 3.10 g pre-mixed Gamborg's salt (Caisson Labs Inc., North Logan, UT, USA), 0.5 g 2-(N-morpholino)ethanesulfonic acid (MES) (USB Products, Affymetrix Inc., Santa Clara, CA, USA), and 800 mL deionized water (pH 5.7, adjusted using 1 M KOH). This was then split evenly into two different bottles, and 4 g agar (USB) was added to both. One bottle received 3% w/v sucrose

(Sigma-Aldrich). Both bottles were then autoclaved, cooled to 55-60°C, and poured into plates.

Seeds were grown in four different plates: two containing Gamborg's medium with sucrose, and two containing medium without sucrose. Ten seeds were placed on each plate, five each of K-8-5 and WT seeds. After chilling at 4°C for 24 hours, the plates were placed in a growth chamber (Percival Environmental Chamber E-30B, Percival Scientific Inc., Boone, IA, USA) under long-day conditions (16 hours light/8 hours dark, 23°C day temperature, 22°C night temperature) and the seeds allowed to germinate and grow.

For procedures not requiring sterile material, plants were grown under both long-day and short-day (8 hours light/16 hours dark) conditions at 23°C. For transmission electron microscopy work, chlorophyll content analysis, and BN-PAGE gels, plants were grown on Jiffy® brand peat pellets under short-day conditions for four weeks, with no fertilizer, before photographing and harvesting. For photosynthesis measurements, used peat pellets were ground up and used to fill Ray Leach Cone-Tainers (model SC-7, Stuewe and Sons Inc., Tangent, OR, USA), into which seeds were then planted. These plants were fertilized every two weeks using Miracle-Gro All-Purpose Plant Food mixed to company specifications (2.75 g/L).

DNA extraction and PCR analysis of genotype

DNA was extracted from leaves and stems of both mutants and WT plants. The tissue was ground using a pellet pestle in a 1.5 mL centrifuge tube in 500 µL extraction buffer (100 mL 0.2 M Tris HCl (USB) at pH 9, 100 mL 0.4 M LiCl (Sigma-Aldrich), 25

mL 25 mM EDTA (USB), 50 mL 1% SDS (USB), and 225 mL deionized water). After centrifuging for 5 minutes at 16,100 x *g* in a microcentrifuge (Eppendorf), the supernatant was removed, spun again, and 400 µL of the new supernatant was placed in a tube containing 400 µL of isopropanol (Sigma-Aldrich). This was mixed, spun again, the supernatant discarded, and the pellet dried. The pellet was gently resuspended in 100 µL of TE buffer by rocking (Maxi-Rotator), and the DNA was then used for PCR.

The primers (ordered from Eurofins MWG Operon, Huntsville, Alabama) used for PCR amplification were the MFP1-RP (5'-TTC TTA TGA GTT CTT CCT TCT GCT GTT TG-3'), MFP1-FP (5'-GGG CTT CTG TGT TCG ATG AAT GTC G-3'), and to amplify the T-DNA insertion, JL-202 (5'-CAT TTT ATA ATA ACG CTG CGG ACA TCT AC-3'). Two WT samples were tested, one with the MFP-FP and MFP-RP primers, and one with the JL-202 and MFP-RP primers. Likewise, two K-8-5 samples were tested, one with the MFP-FP and MFP-RP primers, and one with the JL-202 and MFP-RP primers.

The PCR (using a GeneAmp PCR system 9700 thermocycler, Applied Biosystems, Carlsbad, CA) had an initial melt at 94°C for 5 minutes, followed by 30 cycles consisting of a 30-second denaturing step at 94°C, a 30-second annealing step at 58°C, and a 2-minute extention step at 72°C, with a final extension step at 72°C for 5 minutes. PCR samples were stored overnight at 4°C, and checked the next day on a 1% agarose gel (agarose from National Diagnostics, Atlanta, GA, USA) containing ethidium bromide (USB) to confirm sample genotype.

Transmission Electron Microscopy

Leaf samples taken from four-week-old nonsterile plants were fixed in a 2.5% solution of glutaraldehyde (SPI Supplies, West Chester, PA) in a 1 mM sodium phosphate buffer (pH 6.7) (powders from Sigma-Aldrich), for two weeks to ensure proper tissue infiltration. After two weeks, the glutaraldehyde solution was removed and the samples were washed twice for ten minutes with sodium phosphate buffer. Samples were stained using 1% osmium tetroxide (Ted Pella, Redding, CA) in sodium phosphate buffer for 2 hours, then washed twice for ten minutes in sodium phosphate buffer, followed by dehydration in an ethanol (Sigma-Aldrich) gradient (successively, 50% ethanol for 2 hours, followed by 70%, 85%, and 90% ethanol for 1 hour and 15 minutes each, then in 100% ethanol overnight). Samples were removed from ethanol and soaked twice for seven minutes in propylene oxide (Electron Microscopy Sciences, Hatfield, PA). A 1:1 mixture of propylene oxide and Spurr's Low-Viscosity Resin (SPI Supplies) was prepared, and the samples were soaked in the mixture for 1 hour. After 1 hour, the bottles were opened and the propylene oxide was allowed to evaporate overnight. The next day, the old resin was removed, and enough new resin was added to cover the samples. The leaf tissue was cut into fragments ($\leq$ 3 mm wide) and embedded in flat embedding molds (BEEM brand, Ted Pella) at 70°C for 14-15 hours.

Once hardened, the samples were trimmed with a razor just enough to expose approximately 3 mm of sample. The end of the sample was also trimmed to ensure that the tissue sample was exposed and would be present in microtome slices. Once trimmed, samples were cut on a microtome (Ultracut E Ultramicrotome, Reichert-Jung, Depew, NY) using a glass knife.

Initially, sections were cut at 99 µm, to ensure that the sample face was flat, that the tissue was exposed, and to generate sections to examine under a light microscope. Once the sample face was flat, 99 nm sections were cut for electron microscopy. These 99 nm sections were then placed on 3 mm copper grids, with about five sections of sample per grid, and placed on a piece of filter paper to dry.

Lead citrate stain was prepared fresh using 1.33 g lead nitrate (Electron Microscopy Sciences) and 1.76 g sodium citrate (Electron Microscopy Sciences) mixed in 30 mL distilled water according to the protocol by Reynold (1963). This mixture was shaken vigorously for 1 minute, and allowed to sit for 30 minutes with additional shaking every 5 minutes. After 30 minutes, 8 mL 1 N NaOH (40 g/L) was added, followed by the addition of distilled water to 50 mL. This solution was stored in a 50 mL Falcon tube wrapped tightly in aluminum foil and masking tape to prevent exposure to carbon dioxide and light.

Samples were stained by placing them in a 1% uranyl acetate (Electron Microscopy Sciences) solution for 5 minutes, then rinsed 10x in distilled water. Samples were then stained using lead citrate staining for 5 minutes, and rinsed 10x in CO_2-free distilled water in a container with pellets of sodium hydroxide (Sigma-Aldrich) to prevent the lead from precipitating. After drying samples, they were examined under a JEM-1400 transmission electron microscope (JEOL Ltd., Peabody, MA).

Chlorophyll Count

A single-hole punch was used to punch out three circles of leaf tissue from four-week-old plants (circle area =0.28 cm^2). The circles were incubated in 3 mL N,N-Dimethylformamide (DMF) (Mallinckrodt AR, Paris, Kentucky) for 24 hours in the dark at room temperature to extract the chlorophyll. The absorption was measured on a spectrophotometer (Genesys 20, Thermo Scientific, Waltham, MA). First, the absorption was checked at 420 nm to ensure that the sample wasn't too concentrated (< 0.9), then the instrument was set to absorbance at 720 nm, and the absorbances measured at 470, 647, and 664 nm without resetting the blank between wavelengths (the offset of the blank was recorded at each wavelength instead). Total pigment amounts were calculated using the following equations:

Chlorophyll A (mg/mL): (12 x A664) – (3.11 x A647)

Chlorophyll B (mg/mL): (-4.88 x A664) + (20.78 x A647)

Total Chlorophyll (mg/mL): (7.12 x A664) + (17.67 x A647)

Carotenoids (mg/mL): [(1000 x A470) – (205 x *ChlA*) – (114 x *ChlB*)]/245

Pigment Content (mg/cm^2): (*mg*/*mL*) x (3 mL/0.84 cm^2)

Subsequent statistical analysis was done in SigmaPlot 12.3 (Systat Software, San Jose, CA) using a two-tailed T-test to calculate significance values.

Protein Analysis

Chloroplast isolation was performed using a protocol modified from Kugler et al. (1997). 2.5 g leaf tissue collected from 4-week-old plants was ground in 150 mL ice-cold extraction buffer (330 mM Mannitol (USB), 30 mM HEPES (Calbiochem, EMD

Millipore, Darmstadt, Germany), 3 mM $MgCl_2$ (Sigma-Aldrich), 2 mM EDTA (USB), 0.1% BSA (Sigma-Aldrich) w/v) using a Waring blender set on HIGH for 3 x 10 seconds. The homogenized tissue was poured into labeled bottles for chloroplast isolation at 4°C.

The homogenized tissue was filtered into fresh bottles through four layers of Miracloth (Calbiochem) to remove leaf debris. The solid material was then discarded, and the filtrate centrifuged at 4°C at 2,000 x *g* for 3 minutes in a swinging bucket rotor (Sorvall Legend XTR, rotor 3607, Thermo Scientific). After centrifugation, the supernatant was discarded and the pellet was resuspended in 3 mL extraction buffer.

The resuspended pellet was carefully pipetted onto 25 mL 40% v/v Percoll (Research Organics, Cleveland, OH) solution in extraction buffer, then centrifuged for 30 minutes at 4,815 x *g* in a swinging bucket rotor (Legend XTR, rotor 3607) with the brakes deactivated to prevent the mixing of the two layers.

The intact chloroplasts, located in the bottom layer, were recovered and washed with 20 mL resuspension buffer (extraction buffer without BSA), gently mixed by inversion, and then recentrifuged at 2,500 x *g* for 10 minutes. This step was repeated twice, and the supernatant was discarded.

The protein extraction and BN-PAGE analysis were performed at 4°C according to a protocol modified from Kikuchi et al. (2009). Proteins were extracted from the chloroplast pellet immediately following isolation. The pellet was resuspended in 160 µL solubilization buffer (50 mM Bis-Tris-HCl (Amresco Inc., Solon, OH, USA), pH7; 0.5 M Aminocaproid Acid (Spectrum Chemical, New Brunswick, NJ, USA); 10% w/v Glycerol (USB); 1% w/v water-soluble Digitonin (EMD Millipore); 1% (v/v) protease inhibitor

cocktail for plant extracts (Amresco)) and incubated for 10 minutes. The solution was centrifuged (Eppendorf microcentrifuge) at 16,100 x *g* for 10 minutes, and the supernatant was transferred to new tubes in 80 µL aliquots. Each aliquot received 2 µL CBB-G solution (5% w/v Coomassie Brilliant Blue G-250 (Amresco), 50 mM Bis-Tris HCl pH 7.0, 0.5 M Aminocaproic Acid) and was stored at -20°C.

Proteins were analyzed on a BN-PAGE gel with a gradient of 4% to 14% polyacrylamide, with a 3% stacking gel. The stock solutions were prepared one day before use, and included an acrylamide/bisacrylamide (AB) mix (48% w/v acrylamide (Sigma-Aldrich), 1.5% w/v bisacrylamide (Sigma-Aldrich) in H_2O) and a 3x gel buffer (150 mM Bis-Tris-HCl, pH 7; 1.5 M Aminocaproic Acid). Both solutions were stored at 4 °C. The stock solutions were used to prepare the 4% polyacrylamide (1.2 mL AB, 5 mL 3x gel buffer, water to 15 mL), 14% polyacrylamide (4.2 mL AB, 5 mL 3x gel buffer, 3 g glycerol, water to 15 mL) and stacking gel (364 µL AB, 2 mL 3x gel buffer, water to 6 mL) solutions.

The BN-PAGE gel was prepared using a gradient mixer (GM-100, C.B.S. Scientific Inc., Del Mar, CA) and a peristaltic pump (Pump 60 RPM, VWR Int., Radnor, PA), and the gel was poured into a Bio-Rad 1.5 mm spacer gel plate for the Mini PROTEAN 3 system (Bio-Rad Laboratories, Inc., Hercules, CA). A total of 8 mL gel solution was poured as follows: 4 mL 4% acrylamide solution (with 12.5 µL 10% APS (Sigma-Aldrich) and 1.25 µL TEMED (Sigma-Aldrich)) was added to the chamber furthest from the exit of the gradient pump, and 4 mL 14% acrylamide solution (with 12.5 µL 10% APS and 1.25 µL TEMED) was added to the chamber closest to the exit.

The valve between the two chambers was opened and the pump was turned on to pour the gel. The gel was then overlayed with 100% isopropanol.

The stacking gel was prepared with 2 mL of the stacking gel solution and 12.5 µL 10% APS and 1.25 µL TEMED. The stacking gel mixture was poured into the plate using a glass pipet, and a 1.5 mm 10-well comb was inserted and the gel was allowed to polymerize.

Cathode and anode buffers (1x) were prepared from 10x stock solutions (10x Cathode Buffer: 0.5 M Tricine (Amresco), 150 mM Bis-Tris-HCl, pH 7; 10x Anode Buffer: 0.5 M Bis-Tris-HCl, pH 7). The 1x cathode buffer also received 0.1 g Coomassie Brilliant Blue G-250 per 500 mL. Samples were loaded into wells based on their ultimate use; wells for 1D detection received 20 µL sample; wells for SDS-PAGE received 30 µL sample. Marker wells received 40 µL marker (2 mg/mL equine spleen Ferritin (Sigma-Aldrich) + 0.2 mg/mL BSA in solubilization buffer and CBB-G solution). The gel was run in a Mini-PROTEAN Tetra electrophoresis cell (Bio-Rad Laboratories, Inc., Hercules, CA) at 30V using a 250V power supply (VWR Int., Radnor, PA) at 4°C for 30 minutes, and then raised to 80V for 6 hours.

Immediately after running, the gel was photographed for analysis. The protein complexes represented by the bands were determined by comparing them to other published gels (Fu et al. 2007). The lanes containing 30 µL plant protein extract were then excised and incubated in SDS denaturing buffer (3.3% w/v SDS, 4% v/v 2-mercaptoethanol (Sigma-Aldrich) in 65 mM Tris-HCl, pH 6.8) at 37°C for 30 minutes. The lanes containing the denatured protein were floated in water and pushed gently into SDS-PAGE gels (1.5 mm, 12% running gel, 4% stacking gel, with wells created using a

two-well preparative comb that left space to insert the BN-PAGE gel lane) until they were flush with the stacking gel and no air bubbles were present between the BN-PAGE gel lane and the stacking gel. Any gaps were sealed using a low-melting agarose sealing buffer (0.5% w/v agarose, 25 mM Tris, 192 mM glycine (USB), 0.1% w/v SDS). The gels were run in 1x Tris-Glycine running buffer (0.025 M Tris, 0.192 M Glycine, 0.1% SDS) at room temperature using the 250V power supply, at 80V for 30 minutes followed by 2 hours and 30 minutes at 100V. The finished gels were then used for Western blotting. The lanes loaded with 20 µL protein extract (marker and sample) were excised and incubated in 50 mL SDS denaturing buffer. Proteins from these lanes were used directly for Western blotting.

The blotting gel was incubated for 30 minutes in freshly-made and precooled transfer buffer (2.9 g Glycine, 5.8 g Tris, H_2O to 800 mL, 200 mL methanol (Sigma-Aldrich), 1.85 mL 20% SDS). After incubation, the blotting "sandwich" was assembled as follows: prewetted fiber pad was layered first, followed by prewetted filter paper, then the incubated gel; PVDF membrane (Pall Life Sciences, Port Washington, NY, USA) (wetted in 100% methanol, then rinsed in transfer buffer for 1 minute) was placed on top of the gel, followed by a second piece of prewetted filter paper, and finally the second prewetted fiber pad. The "sandwich" was then closed.

The Western blot apparatus was assembled in the cold room with a cold pack and a constantly running stir bar to keep the solution cool. The blot was run using a 300V power supply (VWR Int., Radnor, PA) at 20V for 15 minutes, then at 100V for 45 minutes. After the blot was complete, the PVDF membrane was removed and marked using a pencil to indicate the protein side of the membrane and the location of the WT, K-

8-5, and marker lanes. The membrane was stained in Ponceau's stain (0.02% w/v Ponceau S (USB), 0.3% w/v trichloroacetic acid (Sigma-Aldrich), 0.3% w/v S-sulfosalicylic acid (Sigma-Aldrich)) for 15 minutes to ensure that the proteins transferred. After the staining, the membrane was destained in deionized water, then incubated overnight at 4°C in blocking buffer prepared with 4 g powdered milk (SACO Foods Inc, Middleton, WI) in 100 mL TBST (1.21 g/L Tris, 8.77 g/L NaCl (USB), 500 µL/L TWEEN, sterile).

The next day, the PVDF membrane was rinsed twice with TBST, then placed into fresh TBST and incubated with shaking at room temperature for 15 minutes. The membrane was then rinsed 2x in fresh TBST for 5 minutes. The TBST was poured off and the MFP1 antibody (OSU-91, 1:5000 in TBST, Jeong et al. 2003) was added and incubated with gentle agitation for 1 hour. After that incubation, the TBST wash steps were repeated as described above. The second antibody was added (Anti-Rabbit IgG (Sigma-Aldrich), 1:10,000 in TBST) and allowed to incubate with gentle agitation for 1 hour. The membrane was washed twice in TBST, incubated in TBST for 15 minutes, then washed 4x5 minutes in TBST. After the final wash step, the old TBST was replaced with fresh buffer before detection.

Detection solution was prepared fresh by combining 1 mL Detection Solution 1 (2.5 mM Luminol (USB), 400 µM p-Coumaric acid (Sigma-Aldrich), 0.1 M Tris-HCl, pH 8.5) with 1 mL Detection Solution 2 (5.4 mM H_2O_2 (Sigma-Aldrich), 0.1 M Tris-HCl, pH 8.5), and the mixture added to a piece of cellophane. The membrane was placed blotted-side down into the detection mix and allowed to incubate for approximately 1 minute, wrapped in fresh cellophane, and exposed to X-Ray film (Blue Ultra Autorad

Film 8x10”, GeneMate, BioExpress, Kaysville, UT) for 15-20 minutes. The exposed film was developed using an X-Ray developer machine (SRX-101A, Konica Minolta, Ramsey, NJ) and allowed to dry.

RESULTS

Lack of MFP1 causes variable phenotypes under differing photoperiods

Plants were examined on a macroscopic scale to determine if there were any deficiencies in growth or changes in color that would be indicative of a loss of photosynthetic efficiency. Seedlings grown from seeds collected in 2001 and 2003 showed a difference in phenotype when grown under a long-day photoperiod, both on plates and on soil (Fig. 1). K-8-5 plants showed delayed growth and bolting compared to the WT, although it eventually did reach maturity and produced seeds alongside the WT. Leaves were noticeably larger and rosettes also appeared denser in the mutant. Plants grown from newer seeds collected in 2009 and 2011 did not display this phenotype when grown under a long-day photoperiod, and both the mutant and WT grew at the same rate and bolted at the same time. However, the newer seeds collected in 2011 showed a slight difference in bolting time when grown under short-day light conditions (Fig. 2). The mutant did not bolt as quickly as the WT, although they did eventually catch up and produce seeds. Plants grown from new seeds showed no notable difference in rosette size between the WT and mutant, and no notable difference in leaf size. There was also no notable difference in the color of the leaves.

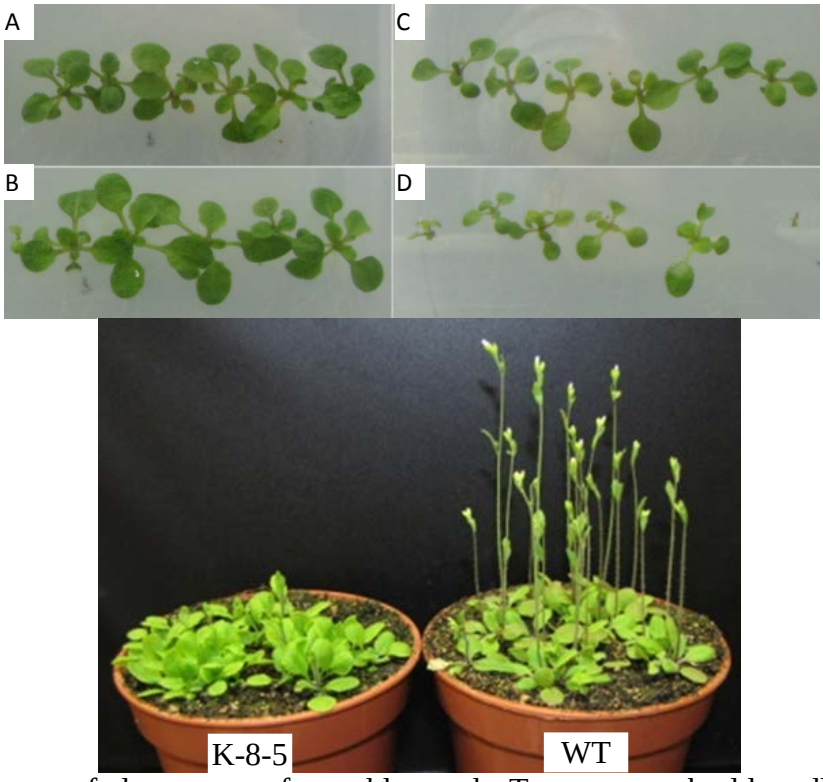

Fig. 1 Phenotype of plants grown from older seeds. Top: two-week-old seedlings on sterile plates. (A) WT seedlings, from seeds collected in 2009. (B) K-8-5 seedlings, from seeds collected in 2009. (C) WT seedlings, from seeds collected in 2001. (D) K-8-5 seedlings, from seeds collected in 2003. Bottom: older, soil-grown plants grown from 2001/2003 seeds.

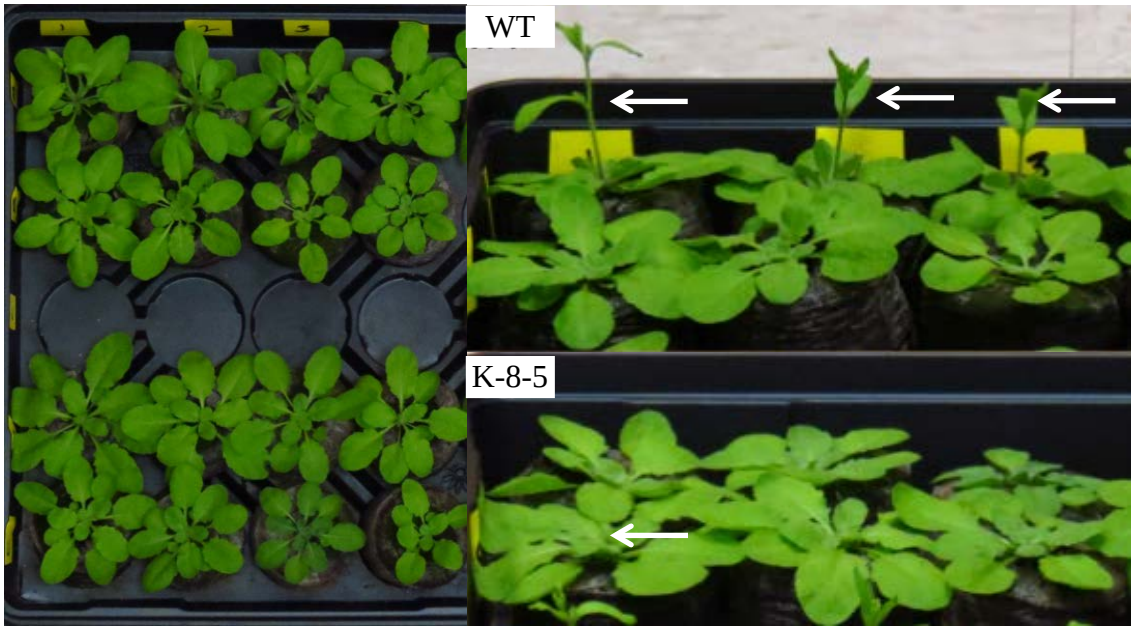

Fig. 2 Four-week-old seedlings grown under short-day conditions. Plants on top are WT, plants on bottom are K-8-5. Arrows are pointing to bolts.

Variability of mutant phenotype was not due to heterozygosity

Because the phenotype of the mutants was inconsistent depending on factors such as the age of the seeds, the soil and medium they were grown in, and the use of fertilizer, it became necessary to analyze the genetic makeup of the plants grown to ensure that they were homozygous mutants and homozygous WT. The forward primers for the MFP1 DNA included one which only amplified the wild-type allele (MFP1-FP), and one which only amplified the mutant allele, as the sequence is derived from the T-DNA insertion (JL-202). Thus, a homozygous WT genome produces bands for the MFP1-FP primer, but not the JL-202 primer, and a mutant genome produces bands for JL-202 primer, but not for the MFP1-FP primer. If bands were present for both the T-DNA insertion and the wild type MFP1 gene, this would indicate the presence of a heterozygote. None of the samples showed two bands indicative of a heterozygote, therefore all samples were homozygous, despite inconsistencies in phenotype (Fig. 3).

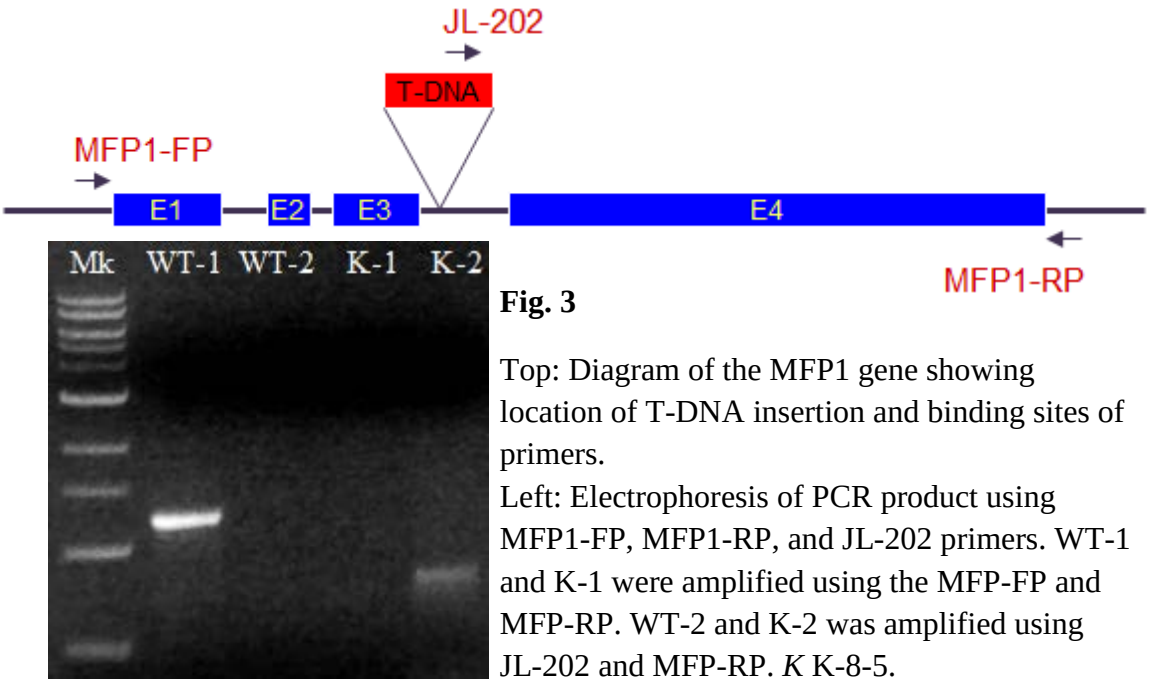

Fig. 3

Top: Diagram of the MFP1 gene showing location of T-DNA insertion and binding sites of primers.
Left: Electrophoresis of PCR product using MFP1-FP, MFP1-RP, and JL-202 primers. WT-1 and K-1 were amplified using the MFP-FP and MFP-RP. WT-2 and K-2 was amplified using JL-202 and MFP-RP. *K* K-8-5.

Mutant thylakoid membranes do not lack grana, but exhibit differences in number of grana stacks and thylakoid layers per granum

Electron microscopy provided a direct view of the thylakoid membranes, as well as a view of any differences in chloroplast shape or size. Electron micrographs of the mutant showed no significant difference in the grana stacking compared to the WT; both plants had healthy, abundant grana stacks with no apparent abnormalities in either (Fig. 4 A-D). There appeared to be a slight difference in chloroplast size; the chloroplasts of the mutant (n = 2) were between 16-30% longer than those of the WT, with the mutant chloroplasts examined being around 6 microns long, whereas the WT chloroplasts (n = 3) were between 4-5 microns long. There were no notable differences in the width of the chloroplasts (Fig. 5 A-D). In addition to the size of the chloroplasts, the number of grana stacks and the number of layers present in the grana stacks were counted. A "grana stack" was considered a section of thylakoid membrane containing

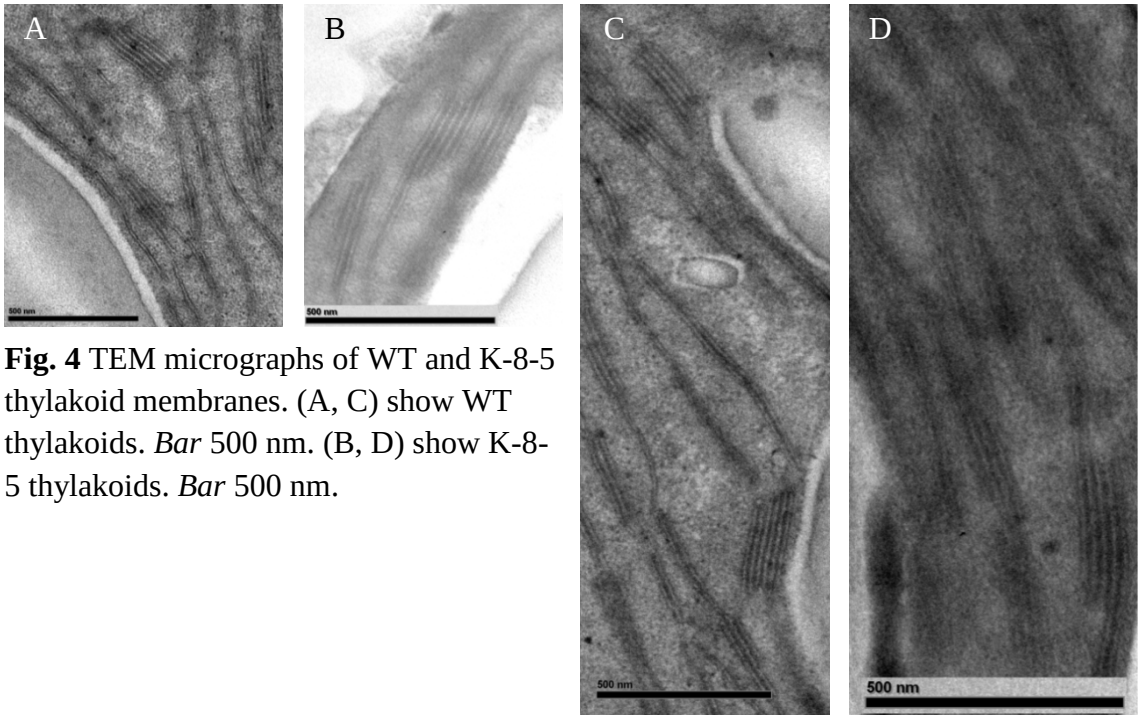

Fig. 4 TEM micrographs of WT and K-8-5 thylakoid membranes. (A, C) show WT thylakoids. *Bar* 500 nm. (B, D) show K-8-5 thylakoids. *Bar* 500 nm.

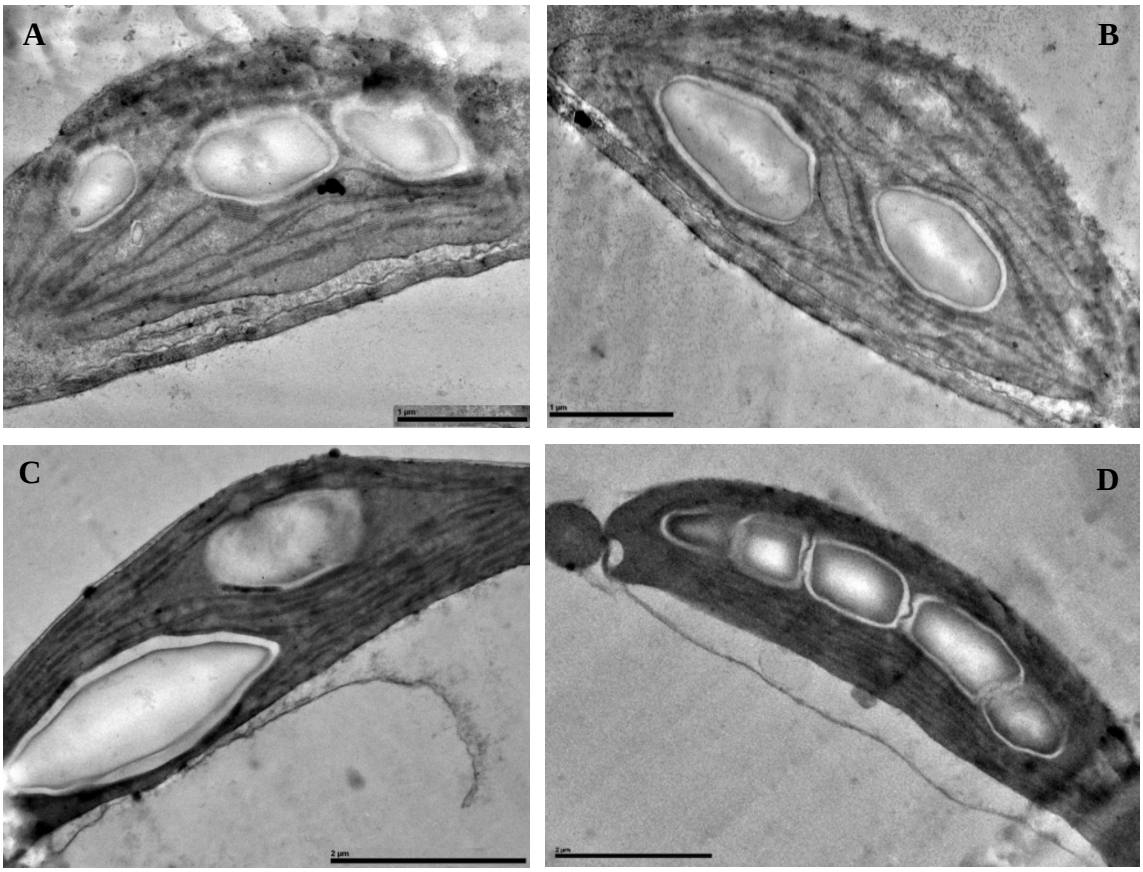

Figure 5 TEM micrographs of WT and K-8-5 chloroplasts. (A, B) show WT chloroplasts. *Bar* 1 µm. (C, D) show K-8-5 chloroplasts. *Bar* 2 µm.

three or more layers; sections with two or fewer layers were not counted as grana stacks. Interestingly, the KO contained a greater number of grana stacks (23.5 stacks/chloroplast, $n = 2$) than the WT (20 stacks/chloroplast, $n = 3$), but the grana stacks in the KO had fewer layers (3.73 layers/granum, $n = 30$) than did the stacks in the WT (4.41 layers/granum, $n = 49$).

Chlorophyll content does not vary significantly in the mutant

Chlorophyll content is an important indicator of the number of photosystems and light harvesting complexes present inside of the plant. Chlorophyll *a* is found in the

reaction centers of both photosystems, and in the light harvesting complex of PSI. Chlorophyll *b* is primarily found in the light harvesting complex of PSII. Thus, adjustments in the ratio of chlorophyll *a* to chlorophyll *b* relative to the WT would indicate an adjustment in the balance of the photosystem complexes themselves.

While there appeared to be an overall trend of increased chlorophyll content in the mutant, the change was not statistically significant and was thus inconclusive (Fig. 6).

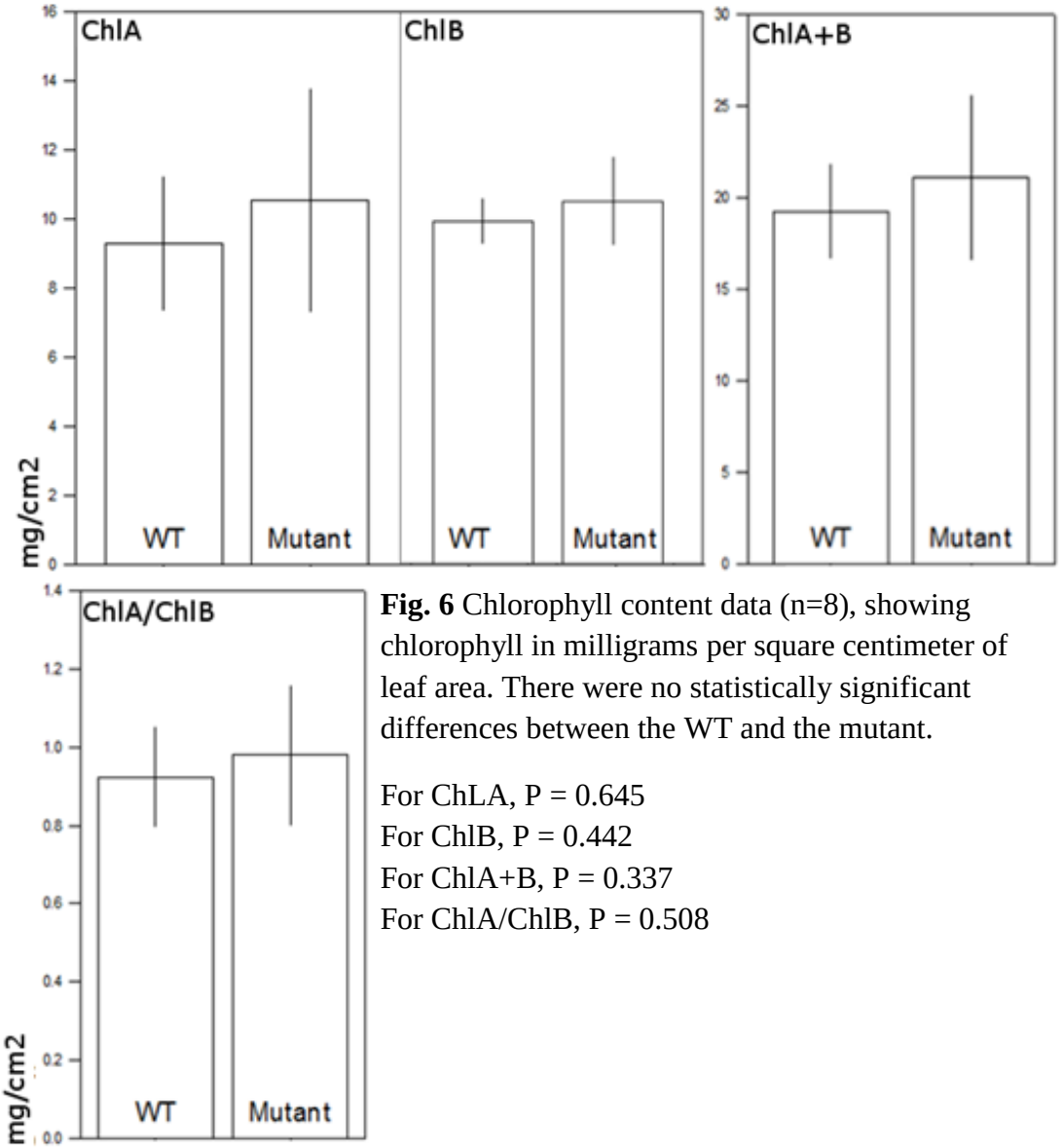

Fig. 6 Chlorophyll content data (n=8), showing chlorophyll in milligrams per square centimeter of leaf area. There were no statistically significant differences between the WT and the mutant.

For ChLA, P = 0.645
For ChlB, P = 0.442
For ChlA+B, P = 0.337
For ChlA/ChlB, P = 0.508

Loss of MFP1 caused changes in protein complex concentrations

Another possibility for MFP1 function was involvement in the formation of protein complexes. The BN-PAGE gel, because it does not denature protein complexes, allowed me to look for potential differences in protein complexes between the WT and the mutant. It also allowed me to detect the MFP1 as it would normally be found inside the cell, whether that is as a homodimer, or as part of a larger complex.

The 1D BN-PAGE gel showed clearly the protein complexes present in the chloroplasts of both the WT and the mutant (Fig. 7). Most bands appeared similar in intensity, however, some bands showed varied intensity between the WT and the K-8-5 samples. The bands located around the 200-300 kDa range, corresponding to the PSII monomers and LHCII-multimers were just barely visible in the mutant when compared to the same bands in the wild type. In addition, a band around 880 kDa, corresponding to PSI and the PSI-LHC supercomplex, appeared more intense than in the WT.

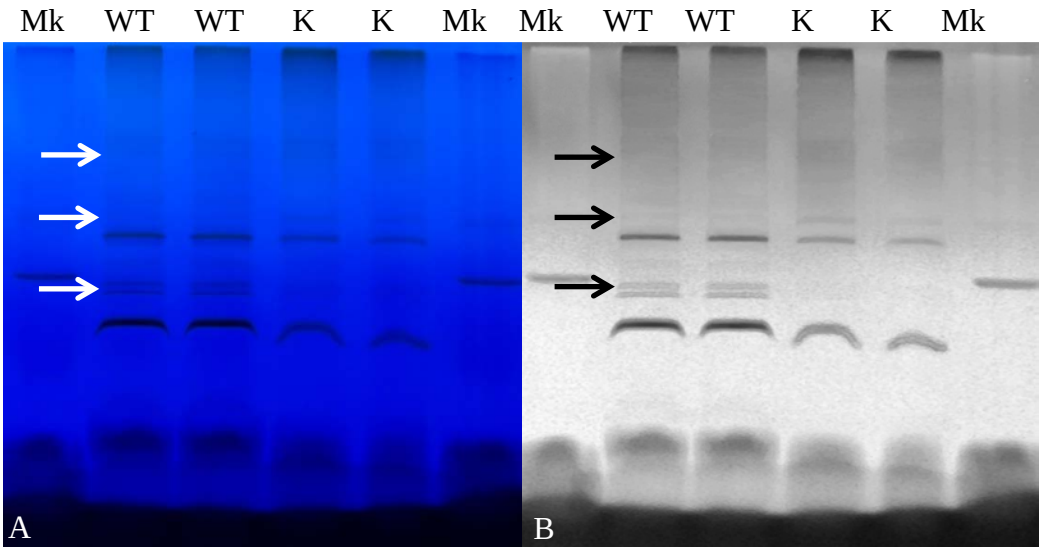

Fig. 7 Appearance of the BN-PAGE gel immediately after running. (A) The 1D BN-PAGE gel as it appeared after removal from running buffer. (B) The same gel, with color digitally removed to highlight areas of varied band intensity. Arrows highlight bands which varied between the WT and K-8-5 samples. *Mk* marker, *K* K-8-5.

MFP1 associates with several specific photosynthetic complexes

The MFP1 protein was detected in WT samples after blotting and immunodetection in both the 1D and 2D BN-PAGE gels. On the 1D BN-PAGE gel (Fig. 8), a strong signal is detected at bands around 160 kDa, with residual signal trailing to 400 kDa, followed by a notable gap, and reappearance of signal above 880 kDa. The lowermost band at 160 kDa corresponded to the LHCII trimer, as well as dimerized MFP1 protein. The band located at 400 kDa corresponds to the location of PSII monomers and the LHC multimers, seen on other gels of the same type performed (Fu et al. 2007). Another strong band was seen above 880 kDa, around the PSII-LHCII supercomplex. No MFP1 signal was detected at less than 160 kDa.

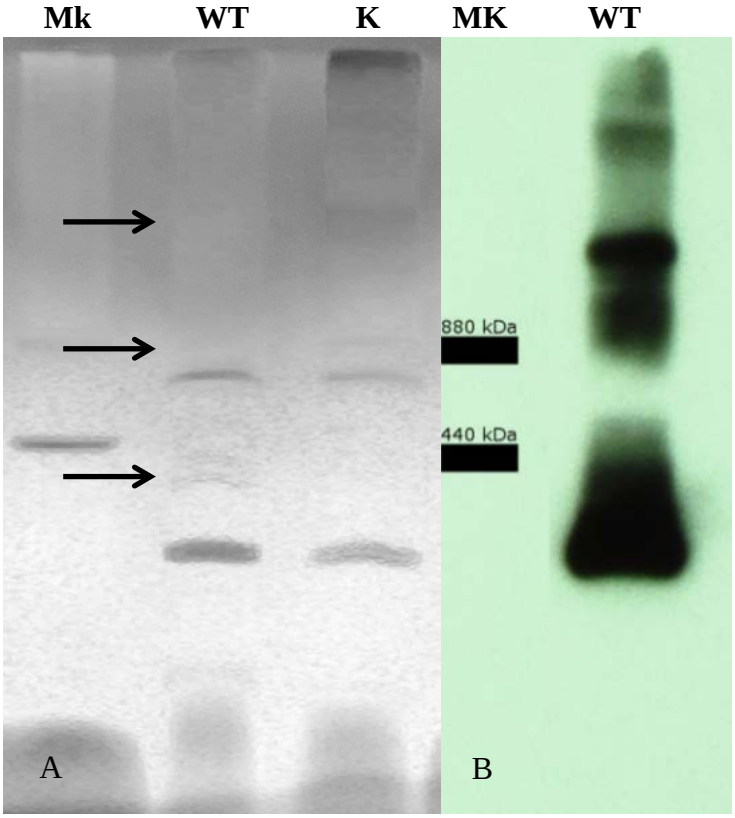

Fig. 8 1D BN-PAGE Western Detection. (A) shows the 1D BN-PAGE gel immediately after the initial run. These lanes were used for (B) the 1D Western Blot. Arrows highlight bands which varied between the WT and K-8-5 samples. *Mk* marker, *K* K-8-5.

On the 2D BN-PAGE gel (Fig. 9), the strongest signals were located at approximately 2D-80 kDa, which is the size of the MFP1 protein, but there is also signal located at points below 2D-80 kDa. The bands of the 1D gel match up with the bands of the 2D gel, with the strongest signal located again at the 1D-160 kDa band. Aside from that band, the strongest signals were again seen around the supercomplexes. Again, there was a lack of signal between 1D-440 kDa and 1D-880 kDa.

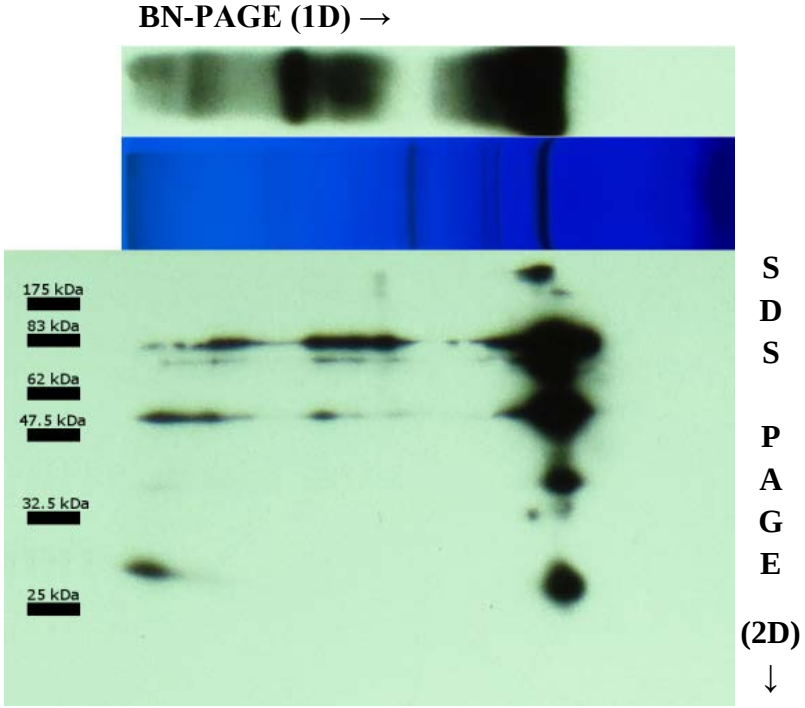

Fig. 9 The 2D BN-PAGE Western Detection, showing strongest MFP1 signal around the region of the dimerized proteins. Signals on the 2D blot (bottom) are lined up with the BN-PAGE gel protein bands and with the 1D BN-PAGE Western Blot (top).

DISCUSSION

The initial hypothesis for the function of MFP1 was that it was involved either in forming or maintaining the structure of the grana stacks. This is due to the protein's structural similarity to that of the golgins, which maintain the stacks in the Golgi apparatus (Rose et al. 2004). The results obtained here, however, do not support this hypothesis. TEM micrographs of the thylakoid membranes of MFP1 knockout plants show no deficiency in thylakoid stacking, nor does the plant suffer when grown under ideal conditions; had thylakoid stacking been deficient, we would have expected knockout plant growth to be affected in all photoperiods due to a loss of photosynthetic efficiency caused by the loss of grana stacks.

TEM micrographs do reveal a slight difference in the number of grana stacks and grana layers. While the difference in the number of layers per granum seem to support the thylakoid stacking hypothesis, this difference could also be due to differences in the numbers of photosystems present in the chloroplasts of the WT versus the MFP1 knockout. If MFP1 were indeed involved in thylakoid stacking specifically, a greater loss of stacking would have been expected.

The difference in the growth of the WT compared to the knockout plants was most notable when grown under a short-day photoperiod. No phenotype was seen when grown under a long-day photoperiod, but a short-day photoperiod caused the phenotype to be expressed in plants grown from new seeds, in the form of a slower bolting time and

a denser rosette. The slow bolting time could be due to a decrease in photosynthetic efficiency, causing the plant to require more time to gather the resources needed for flowering, thus delaying bolting. A denser rosette may make up for the loss in efficiency, since the plant would have more surface area to produce the same amount of product that the WT can produce with less surface area. Another potential explanation for the delay in bolting could be in starch production or lack thereof. It is not currently known if starch content is different in the mutant compared to the WT, and either an increase or a decrease in starch content is possible. Either an increase or decrease in starch accumulation results in a delayed flowering phenotype, as was shown in Arabidopsis mutants that lack starch and others which produce excess starch (Elmert et al. 1995; Corbesier et al. 1998).

The results of the chlorophyll count, while not statistically significant, are interesting nonetheless when other data are taken into account. There appears to be a trend where the mutant shows a decreased ChlA/ChlB ratio comparable to the WT. The percentage of total chlorophyll that is made up of chlorophyll *a* is higher in the mutant than in the WT, and the percentage of total chlorophyll that is made up of chlorophyll *b* is lower in the mutant than in the WT, while total chlorophyll is increased. Chlorophyll *a* is primarily found in the photosystem reaction centers and in the LHCs of PSI. Chlorophyll *b* is primarily found in the LHCs of PSII. If further testing shows that this difference is significant, it could be indicating an alteration of the balance between PSII and PSI, where PSI would be favored. However, since these results were statistically insignificant, further testing needs to be done on the chlorophyll content with a larger sample size before any conclusions can be drawn from this data.

The results of the BN-PAGE experiment were the most telling of a possible function for MFP1. The protein appears to be associated with the PSII-LHCII supercomplexes, of which there is a greater amount in the mutant than in the WT. Though the PSII-LHCII supercomplexes are primarily located in the grana stacks (meaning that MFP1 would also primarily be found there), the presence of stacking seen in the mutant and the lack of phenotypic changes seen in long-day-grown plants indicates that MFP1 does not play a role in grana formation or maintenance. If it did, the phenotype should have been seen in both long- and short-day photoperiods. However, it does indicate that MFP1 may play some role in maintaining the balance of PSII supercomplexes.

It is also interesting that no signal was seen below 160 kDa, indicating that the protein does not exist in the chloroplast as a monomer, but it is always found within a complex or as a dimer with itself. This also indicates that, if MFP1 is associating with LHCII, it is only associating with LHCII in its trimeric form, as opposed to associating with LHCII monomers.

The band at ~160 kDa, and the smearing of signal seen at and above that band, is also of interest. While 160 kDa is the correct size for an MFP1 dimer, this is also the location of the LHCII trimer proteins seen on other BN-PAGE gels (Fu et al. 2007). However, the monomers which make up the LHCII trimer (Lhcb1, Lhcb2, and Lhcb3) are only between 27-30 kDa in size, meaning that the LHCII trimer proper would only be about 90 kDa large (Ruban et al. 1999; Heinemeyer et al. 2004). This size is confirmed in papers which separate the LHCII trimer using methods other than BN-PAGE, which show the LHCII trimer to be between 100-110 kDa in size (Ruban et al. 1999;

Heinemeyer et al. 2004). However, BN-PAGE gels run by other researchers consistently show the LHCII trimer to be around 160 kDa, indicating that something else is associating with the trimer.

Full-length MFP1 is approximately 83 kDa in size; thus, an LHCII bound to an intact MFP1 would be around 190 kDa, still slightly larger than the 160 kDa seen on other BN-PAGE gels. However, since the 2D-SDS-PAGE gel showed MFP1 signal around 50 kDa, corresponding to the LHCII trimer band on the 1D BN-PAGE gel, there may be some amount of cleaved MFP1 that is still associating with the LHCII trimer. This is consistent with previously-run 1D SDS-PAGE gels using Arabidopsis MFP1, which also show a band between 50-65 kDa that most likely corresponds to the coiled-coil domain (Samaniego et al. 2006). This 50 kDa fragment bound to a LHCII trimer would be between 140-160 kDa in size, putting it within the range of the LHCII trimer band.

With the smearing of signal seen on the Western blot, it is likely that MFP1 associates with LHCII trimers in several forms. Firstly, MFP1 is capable of dimerizing, and the detection of both full-length and cleaved MFP1 at the 160 kDa band indicates that it exists in this homodimer form in the cell. Secondly, the cleaved MFP1 binding to LHCII would also put it in the 160 kDa range; the detection of cleaved MFP1 at this location makes this a possibility. Thirdly, the regions above the strongest signal may represent a number of different binding patterns, including LHCII trimers bound to intact MFP1, LHCII trimers bound by multiple MFP1 proteins, variously-sized aggregates of LHCII trimers bound by MFP1, etc. In addition, it is possible that MFP1 only associates

with a specific form of the LHCII trimer (only specific heterotrimers, or only specific homotrimers, of Lhcb1, Lhcb2, and/or Lhcb3).

MFP1 appears to be associated with the LHCII trimer, it is capable of binding DNA, and the loss of MFP1 leads to changes in concentrations of PSII supercomplexes. Taken together, these results suggests that MFP1 could play a role in some form of light response which is not triggered when the plants are grown under ideal lighting conditions. If the phenotype were due strictly to a loss of thylakoid stacking, the difference in phenotype would have been consistent under both short- and long-day conditions.

There are two possibilities for the function of MFP1 that are indicated by these results. Since the levels of these supercomplexes are greater in the mutant, and there is no shift in the location of the bands (indicating little or no change in complex size), MFP1 probably does not play a role in keeping these complexes together or in forming them, as they are still properly formed in the mutant. Rather, it is possible that MFP1 is involved in acclimation to different levels of light, either by the relocation of the LHC during state transition, or in gene regulation during stoichiometry adjustment.

When plants are exposed to light which preferentially excites one photosystem over another, photosynthetic efficiency is decreased; thus, the plant compensates for this by undergoing a state transition, which involves relocating a mobile pool of LHCII from PSII to PSI (Haldrup et al. 2001; Galka et al. 2012). This occurs by phosphorylation of the LHC subunits Lhcb1 and Lhcb2, which grants them a negative charge and forces them out of the grana stacks and into the lamellae, where PSI is primarily concentrated (Haldrup et al. 2001; Galka et al. 2012). MFP1 may aid in the movement of the LHCs

from the grana stacks to the lamellae, perhaps by aiding in the disassociation of the LHCs from PSII. The fact that the bands corresponding to the PSII supercomplexes are stronger in the knockout than in the WT may be evidence for this.

After long periods of exposure to light which preferentially excites one photosystem over another, the plant will adjust the photosystem stoichiometry (the balance of PSII to PSI). If MFP1 is associated with the LHCs, then perhaps the movement of the LHCs (and associated MFP1) during a state transition triggers the transcription of photosystem genes. MFP1 is capable of binding chloroplast DNA and is regulated by phosphorylation by casein kinase II (CKII) (Jeong et al. 2004). This DNA-binding capability may serve several functions in this case: the first possibility is bringing the thylakoid membrane closer to the DNA in order to shorten the distance that the new proteins have to travel; the second is that it may play a role in signaling the chloroplast to produce more photosystem subunits. It is possible that MFP1 may be involved in both. If MFP1 is associated with LHCs in general, then some MFP1 would be located with the PSI-LHCI complex at all times, but the influx of extra LHC may be the trigger that leads to a stoichiometry adjustment. It is also possible that MFP1 only associates with LHCII (Lhcb1, Lhcb2, etc.), and not at all with LHCI. In this case, the movement of LHCII and MFP1 to PSI would expose MFP1's coiled-coil domain to the stroma, allowing it to bind to the nucleoid, and affect gene expression.

Interestingly, phosphorylation is the mechanism which allows state transitioning to occur. Phosphorylation of LHCII by the protein kinase state transition 7 (STN7) results in LHCII being pushed out of the grana and into the lamellae (Haldrup et al. 2001). STN7, however, does not work without being phosphorylated itself; some suggest that

other kinases, such as CKII, may be responsible for phosphorylating STN7 (Willig et al. 2011). It would be interesting to see if any link exists between the phosphorylation of STN7 and of MFP1.

Previous Northern Blot data do not show any difference in chloroplast gene expression between the WT and the MFP1 knockout, however, these experiments were performed using plants grown under ideal light conditions (Jeong 2004). Since the mutant phenotype is induced by short-day photoperiods, it is possible that a repeat of gene expression experiments using plants that display the phenotype would yield different results.

Further studies are required to examine the association, if one does indeed exist, between MFP1 and LHCII and the function of this association. Since the loss of MFP1 leads to delayed flowering, and either an increase or a decrease in starch content can delay flowering, a starch count would provide information on whether the mutant is producing more starch than the WT, or if it is not able to produce as much as the WT (Elmert et al. 1995, Corbesier et al. 1998). If the mutant is producing more starch than the WT, this could indicate that MFP1 plays a role in starch mobilization; if it is producing less, this would be indicative of decreased photosynthetic efficiency. If MFP1 is involved in state transitioning or in photosystem stoichiometry adjustments, photosynthetic efficiency under PSII-favorable light conditions should decrease in the knockout; thus, exposure to PSII-favorable light conditions followed by photosynthetic measurements would provide insight into how well the plant can adapt to differing light conditions. Repetition of the chlorophyll count after inducing a stoichiometry adjustment could also be telling; if a stoichiometry adjustment is taking place, then levels of chlorophyll *b*

would be expected to decrease in proportion to chlorophyll *a*. BN-PAGE analysis on protein extracts from plants exposed to such conditions would also provide insight, as a state change or stoichiometry adjustment would lead to definite changes in band location (due to LHCII movement) or intensity (due to altered PSI/PSII content) that may be absent in the mutant. BN-PAGE on mutants lacking the LHCII trimer could also provide telling data; if MFP1 is associating with LHCII, then a lack of LHCII should result in all MFP1 being detected at the 160 kDa mark, with none around PSII or any other complexes.

It would also be worthwhile to repeat the BN-PAGE analysis using proteins isolated only from thylakoid membranes, instead of total intact chloroplast protein extract. This would eliminate the possibility of MFP1 interacting with proteins located in the stroma. The stroma contains some extremely large protein complexes in the megadalton range which could potentially overlap with the PSII complexes, and smaller proteins that could overlap with the LHCII trimers (Olinares et al. 2010). Though the bands seen on the BN-PAGE gel correspond to those seen on gels run using only thylakoid membrane extract, it would be prudent to exclude the possibility of an overlap in this case.

This study has demonstrated a potential interaction between MFP1, a unique DNA-binding long-coiled-coil plant protein, and LHCII, a light-gathering protein complex vital for photosynthesis. Plants lacking MFP1 show differences in growth and flowering compared to the WT under short-day light conditions, and show a difference in chloroplast size, grana stack number and grana stack size. Analysis of the protein complexes show that the PSII-LHCII supercomplexes are more abundant in the MFP1

knockout than in the WT, and that MFP1 is potentially associated with LHCII trimers, LHCII multimers and the PSII-LHCII supercomplex. This association could implicate MFP1 in either aiding the dissociation of LHCII from PSII during a state transition, or in post-transition signaling that leads to adjustments in photosystem stoichiometry. Both mechanisms are important adaptations which help to maintain photosynthetic efficiency under fluxuating light conditions, and as such, proteins involved in this process are important to plant survival (Galka et al. 2012). Further study is needed to explore these possibilities and further elucidate the role of MFP1 within the chloroplast.

LITERATURE CITED

Albertsson PA (2001) A quantitative model of the domain structure of the photosynthetic membrane. Trends Plant Sci 6:349-353

Allen JF, Forsberg J (2001) Molecular recognition in thylakoid structure and function. Trends Plant Sci 6:317-325

Anderson JM (1982) The role of chlorophyll-protein complexes in the function and structure of chloroplast thylakoids. Mol Cell Biochem 46:161-172

Anderson JM, Melis A (1983) Localization of different photosystems in separate regions of chloroplast membranes. Proc Natl Acad Sci USA 80:745-749

Bald D, Kruip J, Rogner M (1996) Supramolecular architecture of cyanobacterial thylakoid membranes: How is the phycobilisome connected with the photosystems? Photosynth Res 49:103-118

Barr FA, Short B (2003) Golgins in the structure and dynamics of the Golgi apparatus. Curr Opin Cell Biol 15:405–413

Cattolico, RA (1986) Chloroplast evolution in algae and land plants. Tree 1:64-67.

Cavalier-Smith, T (2002) Chloroplast evolution: secondary symbiogenesis and multiple losses. Curr Biol 12:62-64

Corbosier L, Lejeune P, Bernier G (1998) The role of carbohydrates in the induction of fowering in *Arabidopsis thaliana*: comparison between the wild type and a starchless mutant. Planta 206:131-137

Cui YL, Jia QS, Yin QQ, Lin GN, Kong MM, Yang ZN (2011) The GDC1 gene encodes a novel ankyrin domain-containing protein that is essential for grana formation in *Arabidopsis*. Plant Physiol 155:130-141

Elmert K, Wang SM, Lue WL, Chen J (1995) Monogenic recessive mutations causing late floral initiation and excess starch accumulation in *Arabidopsis*. Plant Cell 7:1703-1712

Fu A, He Z, Cho HS, Lima A, Buchanan BB, Luan S (2007) A chloroplast cyclophilin functions in the assembly and maintenance of photosystem II in *Arabidopsis thaliana*. Proc Natl Acad Sci USA 104:15947-15952

Galka P, Santabarbara S, Khuong TTH, Degand H, Morsomme P, Jennings RC, Boekema EJ, Caffarri S (2012) Functional analyses of the plant photosystem I–light-harvesting complex II supercomplex reveal that light-harvesting complex II loosely bound to photosystem II is a very efficient antenna for photosystem I in state II. Plant Cell 24:2963-2978

Gindullis F, Meier I (1999) Matrix attachment region binding protein MFP1 is localized in discrete domains at the nuclear envelope. Plant Cell 11:1117-1128

Giovannoni SJ, Turner S, Olsen GJ, Barns S, Layne DJ, Pace NR (1988) Evolutionary relationships among cyanobacteria and green chloroplasts. J Bacteriol 170:3584-3592

Gounaris K, Barber J, Harwood JL (1986) The thylakoid membranes of higher plant chloroplasts. J Biochem 237:313-326

Haldrup A, Jensen PE, Lunde C, Scheller HV (2001) Balance of power: a view of the mechanism of photosynthetic state transitions. Trends Plant Sci. 6:301-305.

Harder PA, Silverstein RA, Meier I (2000) Conservation of matrix attachment region-binding filament-like protein 1 among higher plants. Plant Physiol 122:225-234

Heinemeyer J, Eubel H, Wehmhoner D, Jansch L, Braun HP (2004) Proteomic approach to characterize the supramolecular organization of photosystems in higher plants. Phytochem 65:1683-1692

Hoober J, Eggink L (1999) Assembly of light-harvesting complex II and biogenesis of thylakoid membranes in chloroplasts. Photosynth Res 61:197-215

Jaynes JM, Vernon LP (1982) The cyanelle of *Cyanophora paradoxa*: almost a cyanobacterial chloroplast. Trends Biochem Sci 3376:22-24

Jeong SY (2004) Functional investigation of Arabidopsis long coiled-coil proteins and subcellular localization of plant Ran-GAP1. Ph D Thesis, The Ohio State University

Jeong SY, Peffer N, Meier I (2004) Phosphorylation by protein kinase CKII modulates the DNA-binding activity of a chloroplast nucleoid-associated protein. Planta 219:298–302

Jeong SY, Rose A, Meier I (2003) MFP1 is a thylakoid-associated, nucleoid-binding protein with a coiled-coil structure. Nucleic Acids Res 17:5175-85

Kikuchi S, Oishi M, Hirabayashi Y, Lee DW, Hwang I, Nakai M (2009) A 1-megadalton translocation complex containing Tic20 and Tic21 mediates chloroplast protein import at the inner envelope membrane. Plant Cell 21: 1781-1797

Kobayashi K, Kondo M, Fukuda H, Nishimura M, Ohta H (2007) Galactolipid synthesis in chloroplast inner envelope is essential for proper thylakoid biogenesis, photosynthesis, and embryogenesis. Proc Natl Acad Sci USA 104:43

Kramer P, Wilhelm C, Wild A, Morschel E, Rhiel E (1988) Ultrastructure and freeze-fracture studies of the thylakoids of *Mantoniella squamata* (*Prasinophyceae*). Protoplasma 147:170-177

Kroll D, Meierhoff K, Bechtold N, Kinoshita N, Westphal S, Vothknecht U, Soll J, Westhoff P (2000) VIPP1, a nuclear gene of *Arabidopsis thaliana* essential for thylakoid membrane formation. Proc Natl Acad Sci USA 98:4238-4242

Kugler M, Jansch L, Kruft V, Schmitz UK, Braun HP (1997) Analysis of the chloroplast protein complexes by blue-native polyacrylamide gel electrophoresis (BN-PAGE). Photosynth Res 53:35-44

Lemieux C, Otis C, Turmel M (1999) Ancestral chloroplast genome in *Mesostigma viride* reveals an early branch of green plant evolution. Nature 403:649-652

Mamedov MD, Hayashi H, Wada H, Mohanty PS, Papageorgiou GC, Murata N (1991) Glycinebetaine enhances and stabilizes the evolution of oxygen and the synthesis of ATP by cyanobacterial thylakoid membranes. Fed Eur Biochem Soc 294:271-274

Martin M, Rujan T, Richly E, Hansen A, Cornelsen S, Lins T, Leister D, Stoebe B, Hasegawa M, Penny D (2002) Evolutionary analysis of *Arabidopsis*, cyanobacterial, and chloroplast genomes reveals plastid phylogeny and thousands of cyanobacterial genes in the nucleus. Proc Natl Acad Sci USA 99:12246–12251

Martin W, Stoebe B, Goremykin V, Hansmann S, Hasegawa M, Kowallik KV (1998) Gene transfer to the nucleus and the evolution of chloroplasts. Nature 393:162-165

National Center for Biotechnology Information, http://www.ncbi.nlm.nih.gov/. Accessed 25 February 2010

Olinares PDB, Ponnala L, van Wijk KJ (2010) Megadalton complexes in the chloroplast stroma of *Arabidopsis thaliana* characterized by size exclusion chromatography, mass spectrometry, and hierarchical clustering. Mol and Cell Proteomics 9:1594-1615

Peltier JB, Ytterberg AJ, Sun Q, Van Wijk K (2004) New functions of the thylakoid membrane proteome of *Arabidopsis thaliana* revealed by a simple, fast, and versatile fractionation strategy. J Biol Chem 279:49367–49383

Pfeiffer S, Krupinska K (2005) New insights in thylakoid membrane organization. Plant Cell Physiol. 46:1443–1451

Raven JA (2002) Carboxysomes and peptidoglycan walls of cyanelles: possible physiological functions. Eur J Phycol 38:47-53

Raven JA, Allen JF (2003) Genomics and chloroplast evolution: what did cyanobacteria do for plants? Genome Biol 4:209-214

Reynold, ES (1963) The use of lead citrate at high pH as an electron-opague stain in electron microscopy. J Cell Biol 17:208-213

Rippka R, Waterbury J, Cohen-Bazire G (1974) A cyanobacterium which lacks thylakoids. Archaeolog Microbiol 100, 419-436

Rose A, Manikantan S, Schraegle SJ, Maloy MA, Stahlberg EA, Meier I (2004) Genome-wide identification of *Arabidopsis* coiled-coil proteins and establishment of the ARABI-COIL database. Plant Physiol 134:927-939

Rose A, Meier I (2004) Scaffolds, levers, rods and springs: diverse cellular functions of long coiled-coil proteins. Cell Mol Life Sci 61:1996–2009

Ruban AV, Lee PJ, Wentworth M, Young AJ, Horton P (1999) Determination of the stoichiometry and strength of binding of xanthophylls to the photosystem II light harvesting complexes. J Biol Chem 15:10458–10465

Samaniego R, de la Torre C, Moreno Díaz de la Espina S (2008) Characterization, expression and subcellular distribution of a novel MFP1 (matrix attachment region-binding filament-like protein 1) in onion. Protoplasma 233:31-38

Samaniego R, Jeong SY, Meier I, Moreno Díaz de la Espina S (2006) Dual location of MAR-binding, filament-like protein 1 in *Arabidopsis*, tobacco, and tomato. Planta 223:1201–1206

Schubert M, Petersson UA, Haas BJ, Funk C, Schroder WP, Kieselbach T (2002) Proteome map of the chloroplast lumen of *Arabidopsis thaliana*. J Biol Chem 277:8354-8365

Sharkey TD (1985) Photosynthesis in intact leaves of C3 plants: physics, physiology and rate limitations. Bot Rev 51:53-105

Shih MC, Lazar G, Goodman HM (1986) Evidence in favor of the symbiotic origin of chloroplasts: primary structure and evolution of tobacco glyceraldehyde-3-phosphate dehydrogenases. Cell 47:73-80

Shimoni E, Rav-Hon O, Ohad I, Brumfeld V, Reich Z (2005) Three-dimensional organization of higher-plant chloroplast thylakoid membranes revealed by electron tomography. Plant Cell 17:2580–2586

Short B, Haas A, Barr FA (2004) Golgins and GTPases, giving identity and structure to the Golgi apparatus. Biochim Biophys Acta 1744, 383–395

Simpson DJ, Wettstein DV (1989) The structure and function of the thylakoid membrane. Carlsberg Research Communications 54:55-65

Tester M, Blatt MR (1989) Direct measurement of K+ channels in thylakoid membranes by incorporation of vesicles into planar lipid bilayers. Plant Physiol 91:249-252

Trissl HW, Wilhelm C (2002) Why do thylakoid membranes from higher plants form grana stacks? Trends Biochem Sci 18:415-419

Vothknecht UC, Westhoff P (2001) Biogenesis and origin of thylakoid membranes. Biochim Biophys Acta 1541:91-101

Willig A, Shapiguzov A, Goldschmidt-Clermont M, Rochaix JD (2011) The phosphorylation status of the chloroplast protein kinase STN7 of *Arabidopsis* affects its turnover. Am Soc Plant Biol 157:2102-2107

Wolff C, Roy S, Ingham PW (2004) Multiple muscle cell identities induced by distinct levels and timing of hedgehog activity in the zebrafish embryo. Genes Dev 18:1565–1576

BIOGRAPHY

Amanda Rose Havighorst was born in 1987 to William and Karen Havighorst in West Islip, New York. In 2004 her family relocated to western North Carolina, where she was accepted to Western Carolina University in 2005. Within her first year there she declared her major in biology, and she received her Bachelor's degree in Biology in 2009. She continued to Appalachian State University in pursuit of a Master's degree in Biology, where she worked in the laboratory of Dr. Annkatrin Rose and received her Master of Science in 2012. She currently plans to continue her education and pursue a Ph.D, after which she hopes to continue doing molecular research on plants.